

# The Preparation and Tensile Properties of Polyethylene Composites

W. T. MEAD and ROGER S. PORTER, *Polymer Science and Engineering Department, Materials Research Laboratory, University of Massachusetts, Amherst, Massachusetts 01003*

## Synopsis

Single polymer composites have been prepared using different morphologies of polyethylene as matrix and as the reinforcement. Depending on annealing conditions, the ultraoriented fibers used as reinforcement can have higher melting points (ca. 139°C) than the matrix made from the same conventionally crystallized high-density polyethylene (ca. 132°C) or from low-density polyethylene (ca. 110°C). The optimum temperature has been assessed for bonding to occur by growth of transcrystalline regions from the melt matrix without considerable modulus reduction of the annealed ultraoriented and reinforcement fiber or film. Pullout tests have been used for determining the interfacial shear strength of these single polymer composites. The interfacial shear strength for the high-density polyethylene films embedded in a low-density polyethylene matrix is 7.5 MPa and for high-density polyethylene self-composites is 17 MPa. These values are greater than the strength for glass-reinforced resins. The strength is mainly due to the unique epitaxial bonding which gives greater adhesion than the compressive and radial stresses arising from the differential shrinkage of matrix and reinforcement. The tensile modulus of composites prepared from uniaxial and continuous high-density polyethylene films embedded in low-density polyethylene obeys the simple law of mixtures and the reinforced low-density polyethylene modulus is increased by a factor of 10. High strength cross-ply high-density-polyethylene-low-density-polyethylene laminates have also been prepared and the mechanical properties have been studied as the film orientation is varied with respect to the tensile axis.

## INTRODUCTION

Great strength enhancement and resistance to fracture can be obtained when a high strength fiber is used to reinforce a low strength polymer matrix. Ultraoriented and high modulus (ca. 70 GPa) high-density polyethylene (HDPE) fibers and film strips have already been prepared in this laboratory by solid state extrusion in an Instron Capillary Rheometer.<sup>1,2</sup> The higher nylons have also been prepared in this ultraoriented form by solid state extrusion.<sup>3</sup> Consequently, it has been possible to prepare composites from a single polymer by using a difference in melting points between a matrix and a thermodynamically more stable ultraoriented chain-extended crystal form of the thermoplastic.

Capiati and Porter<sup>4</sup> showed that a very high interfacial shear strength of 17 MPa was achievable for HDPE self-reinforcement. This value is greater than the bonding strength for glass-reinforced polyesters and is due to the unique epitaxial bonding rather than the radial forces from compressive shrinkage. The temperature at which the HDPE fiber was embedded in the matrix was 139°C.

Recent work has shown<sup>5</sup> that the ultradrawn HDPE fibers undergo structural reorganization at annealing temperatures as low as 132°C, the ambient melting of the conventionally crystallized HDPE. However, annealing of laterally

constrained fibers below 135°C does not result in structural changes as detected by differential scanning calorimetry. This is possibly a result of constraining the morphology, thus reducing entropy changes and increasing the melting point. This distinction of applying a lateral constraint is crucial since fiber annealing decreased the tensile modulus from 70 GPa towards the 1 GPa observed for the unoriented HDPE. Thus the temperature for preparing the single-polymer composites is chosen to insure a high surface energy, promoting matrix nucleation, epitaxial crystal growth and increased perfection in bonding between matrix and fiber. The embedding temperature, however, must be low enough to avoid a significant decrease of modulus during annealing.

In the present study a low-density polyethylene (LDPE) and HDPE is used as the matrix while ultraoriented films and fibers of HDPE are used as reinforcement. Thus the composite modulus can be increased dramatically over that of the matrix. The interfacial shear strength of these new composites has been studied as well as the mechanical properties of uniaxial and continuous HDPE fibers and film strips embedded in a HDPE and LDPE matrix. The properties of cross-ply laminates have also been considered.

## EXPERIMENTAL

The high modulus high-density polyethylene prepared in this and in previous studies by solid-state extrusion was DuPont alathon 7050 which has weight and number average molecular weights of 58,000 and 18,400.<sup>1</sup> The material used as matrix for the composites was the HDPE and Alathon 2820 LDPE with a melt index of 23 and a density of 0.916 g cm<sup>-3</sup>.

To extrude the high modulus films and fibers, stainless-steel dies were used, with a wedge-shaped die for the films and a conical die for the fibers. The entrance width of the wedge decreased over a distance of 2.8 cm from 0.8 ( $2b$ ) to 0.045 cm ( $t$ ) (equations using these symbols are given below), equal to the thickness of the thin film produced by extrusion through the die. A second die was used with an initial inset width of 0.8 cm ( $2b$ ) decreasing at an angle of 16.7° ( $\theta_1$ ) to the extrusion axis to a width of 0.2 cm ( $2c$ ).  $c$  then decreased at an angle of 7.1° ( $\theta_2$ ) to the extrusion axis until the width of the die inset was equal to the film thickness. The geometry of the conical die and its draw ratio variation have been described elsewhere.<sup>5,6</sup> The dies were polished and cleaned with acetone.

The fibers and films were prepared according to the details now described elsewhere.<sup>1,6</sup> No lubricant was used for the extrusion. The crystallization and extrusion temperature and pressures were 134°C and 0.23 GPa, respectively. An Instron testing machine model TTM was used for the tensile modulus and strength measurements. The tensile modulus was determined by the tangent to the stress-strain curve at a strain level of 0.1%. A strain gauge extensometer was used and each modulus measurement was an average of the modulus variation of the fiber over the length of the strain gauge, equal to 2.5 cm. The aspect ratio of the film strips was ca. 300 so that no end correction was necessary for the modulus data.<sup>7</sup> The tensile strength and modulus measurements were conducted at room temperature at engineering strain rates of  $2 \times 10^{-3}$  and  $2 \times 10^{-4}$  sec<sup>-1</sup>.

The interfacial shear strength of the composite was evaluated by a method described by Capiati and Porter<sup>4</sup> except that no pressure was maintained on the

fiber/matrix system to avoid laterally constraining the fiber and thus prevent necessary structural reorganization of the fiber surface for bonding and epitaxial growth. Further, the fibers were annealed for twenty minutes prior to cooling the composites at ca.  $1^{\circ}\text{C min}^{-1}$  to room temperature. Composites were also prepared by placing the fibers or thin films in a press (PHI, California). The temperature of the mold was  $130^{\circ}\text{C}$ , unless otherwise stated, and was monitored with thermocouples placed into holes drilled into the mold near the specimen. The composites were heated for 30 min unless otherwise stated. Dumbbell-shaped composites were prepared with a cross-sectional area of  $1.27 \times 0.3$  cm, and other thicknesses necessary to vary the volume fraction of fiber content. The high modulus fibers and films of HDPE were cleaned by dipping them in acetone at room temperature.

## RESULTS AND DISCUSSION

### Mechanical Properties of Annealed HDPE Fibers

The annealing characteristics of the ultraoriented fibers have been reported elsewhere.<sup>5</sup> The reinforcing fibers on annealing (applying no lateral constraint and using annealing temperatures above  $126^{\circ}\text{C}$ ) can themselves become composites consisting of an ultraoriented and high melting point (ca.  $139^{\circ}\text{C}$  at  $10^{\circ}\text{C min}^{-1}$  heating rate) fiber core retaining the properties of the original fiber, surrounded by a matrix having a melting point ca.  $7^{\circ}\text{C}$  lower than the core. The matrix has a lower degree of orientation and crystallinity than the fiber and has a morphology with possible chain-fold content and degree of crystallinity similar to the original HDPE used prior to the solid state extrusion. The mechanical properties of the annealed fibers are of importance since they are composites with an ideal morphology gradient from fiber to matrix. The problem of producing epitaxial growth from two different clean polyethylene surfaces is thus avoided.

For laterally constrained fibers, the modes of deformation of the HDPE constrained fibers (i.e., fibers placed in a steel tube equal to their diameter) heated for 1 hr at successive temperatures from  $134^{\circ}$  to  $139^{\circ}$  have also been evaluated. Above  $135^{\circ}\text{C}$  the initial tangent modulus and ultimate strength of the fiber rapidly decrease as the temperature of the fiber approaches  $139^{\circ}\text{C}$ . The extent to which the annealed fiber had undergone structural reorganization is estimated by the parameter  $W_F$ , the weight fraction of structurally reorganized fiber.<sup>5</sup>  $W_F$  increases approximately exponentially with temperature. As the temperature of the constrained fiber is increased from  $135^{\circ}$  to  $139^{\circ}\text{C}$ ,  $W_F$  varies from zero to unity. As  $W_F$  varies from zero to unity, the fiber modulus decreases from ca. 70 GPa to the tensile modulus of an unoriented HDPE, 1 GPa, as shown in Figure 1.

$W_F$  may also be defined in terms of the volume fraction of fiber, assuming the matrix and fiber form separate phases of density  $d_M$  and  $d_F$ , respectively.

The volume fraction of fiber is

$$V_F = \frac{1 - W_F}{1 + W_F(d_F/d_M - 1)} \quad (1)$$

The data of tensile modulus vs  $W_F$  or  $V_F$  is shown in Figure 1. The data of tensile modulus vs  $W_F$  for  $W_F > 0.1$  may be represented by a law of mixtures

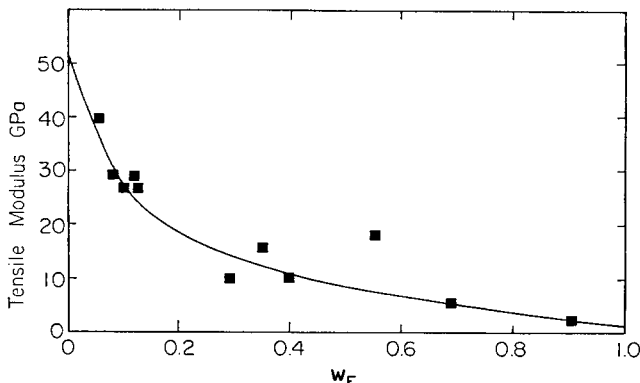


Fig. 1. Tensile modulus of annealed ultraoriented HDPE fibers vs  $W_F$  or  $V_F$ , the volume fraction of fiber.

[as given by eq. (9)]. The discrepancy of the modulus data from the law of mixtures for  $W_F < 0.1$  may be due to the variation of  $V_F$  with  $W_F$  since  $d_F/d_M$  is of the order of one and  $V_F \sim (1 - W_F)^2$ . As  $W_F$  approaches zero, the assumption that two distinct phases are formed may not be valid. The modulus of the ultradrawn fiber will also be a function of the crystal aspect ratio as discussed in more detail elsewhere.<sup>5,8</sup>

A brittle mode of deformation was observed for fibers annealed at 135°C. The extension to fracture was of the order of (3–5)%, the modulus was  $\sim 70$  GPa and the fracture surface consisted of long “needlelike” fibrils. A cold drawing mode of deformation was observed after annealing the fiber at 138°C. This mode was associated with local yielding and an extension to fracture of the order of 200%. The drawn HDPE has a melting point of 138°C at a heating rate of 10°C.

The radial thickness  $\Delta r$  of the structurally reorganized outer surface of the annealed fiber (of radius  $r$  equal to 0.066 cm) may be estimated. For ease of computation, it has been assumed that the melted fiber forms a distinct separate phase, then

$$\Delta r = r(1 - V_F^{1/2}) \quad (2)$$

Since the time and temperature dependence of  $W_F$  have already been estimated,<sup>5</sup> the time and temperature dependence of the melted region may also be deduced from eqs. (1) and (2). Equation (2) shows that for laterally constrained fibers heated below 135°C when  $W_F$  is zero,  $V_F$  is unity, and  $\Delta r$  equals zero. Hence composites prepared by embedding laterally constrained fibers (i.e., embedding the fibers under high pressure) in the matrix below 135°C will have low interfacial strength arising only from the radial stresses which exist across the interface and which are estimated in the following subsection. If the thickness of the annealed fiber required to form epitaxial growth is 1  $\mu\text{m}$ , then  $W_F$  must be greater than  $2 \times 10^{-3}$  or  $V_F$  must be less than 0.998. The embedding temperature must also be sufficiently high to produce a high surface energy promoting epitaxial growth without significantly reducing the mechanical properties of the fibers. HDPE composites having a desired morphology gradient and bonding can be directly prepared by extrusion at temperatures higher than 134°C whereas HDPE/LDPE composites were also prepared by coextrusion.

### Evaluation of Interfacial Bonding

A key to understanding the tensile properties of the composites is the elucidation of the nature of the composite components. The ultraoriented polyethylene fibers have heretofore been subjected to intense characterization.<sup>1-6</sup> The thermal properties of the fibers as they are annealed to form composites have already been discussed,<sup>5</sup> while the time dependence of the birefringence of the annealed fibers will be reported elsewhere.<sup>9</sup>

In this section a study is made to deduce the annealing temperature at which adhesion between matrix and fiber is a maximum and where the fiber annealing and structural reorganization is a minimum. The following experiments were therefore conducted.

A system, as devised by Kelly and Tyson,<sup>10</sup> was used and developed by Capiati and Porter<sup>4</sup> for studying the interfacial strength of fibers and films embedded in a matrix. The strength of the matrix-fiber interface is measured by fiber pullout experiments at constant strain rate. The pullout stresses are measured on fibers embedded to various lengths in the matrix. The average interfacial shear stress  $\tau_{AV}$  is defined as the pullout force divided by the lateral area of the embedded fiber.

Figure 2 plots  $\tau_{AV}$  vs  $T_E$ , the temperature at which the fiber was embedded into the matrix. The embedded fiber length was 1 cm. The draw ratio variation along the fiber was only 25-30. The annealing characteristics of the fibers are draw ratio dependent.<sup>5</sup> The temperature range used for the HDPE/LDPE coextrusion was 115°C, i.e., from 5°C above the melting point of the LDPE to 139°C, the melting point of the constrained HDPE fiber. At 115°C the pullout force is less than 0.2 MPa and there is apparently no bonding between matrix and fiber. As the embedding temperature  $T_E$  is increased,  $\tau_{AV}$  rises. The increase of  $\tau_{AV}$  does not uniquely prove that there is epitaxial bonding since the

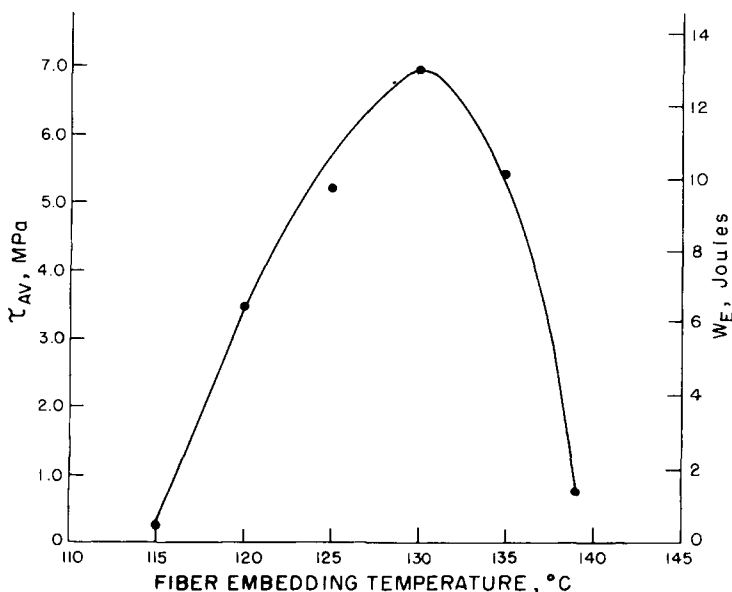


Fig. 2.  $\tau_{AV}$ , the average interfacial shear strength of the polyethylene composite bonding as a function of fiber embedding temperature. Embedded fiber length is 1 cm.

bond strength could also be due, in part, to compressive forces arising from cooling the composite from the embedding temperature  $T_E$  to room temperature  $T_R$ , i.e.,

$$\tau_{AV} = k \Delta\alpha \Delta T \quad (3)$$

where

$$\Delta\alpha = |\alpha_M - \alpha_{\perp}|$$

and

$$\Delta T = T_E - T_R$$

where  $k$  is proportional to the modulus of the matrix,  $\alpha_M$  and  $\alpha_{\perp}$  are the expansion coefficients of the matrix and fiber perpendicular to the axis.  $\tau_{AV}$  will therefore be proportional to the embedding temperature due solely to the contractive forces. In Figure 2 the work done in pulling out the fiber from the matrix is also evaluated:

$$W_E = \left( \frac{\tau_{AV} \pi d}{2} \right) L_E^2 \quad (4)$$

where  $d$  is the fiber diameter and  $L_E$  is the fiber length embedded in the matrix.

The embedding temperature where  $\tau_{AV}$  is a maximum will depend on the lateral constraint applied to the fiber. If the fiber is constrained, a higher embedding temperature will be required (ca. 139°C) for high interfacial strength. Hence by constraining the fiber it is possible to produce a HDPE self-composite. The ultraoriented HDPE fibers or films undergo structural reorganization above 135°C while the HDPE matrix has a melting point of 132°C. Capiati and Porter<sup>4</sup> obtained a value of 17 MPa for the interfacial shear strength of HDPE self-composites. This may not be the maximum obtainable value for such composites, even though the strength is greater than for glass-reinforced fibers. The embedding temperature where  $\tau_{AV}$  is a maximum will also depend on the annealing time but this may not be crucial once the outer surface of the fiber is annealed to form a bond with the matrix.

In the region 130°–135°C, epitaxial bonding appears to occur as shown by the maximum of  $\tau_{AV}$  vs  $T_E$ . Bonding is expected to occur in this range since laterally unconstrained fibers structurally reorganize near ~130°C. At 139°C the annealed fibers necked at the fiber-matrix interface during the pullout test. This explains why the strain to fracture of the bond, shown in Figure 3, rapidly increases with embedding temperature. The strain to fracture of the bond was deduced from the stress-strain curve in which the stress rapidly decreased followed by the fiber pulling out of the matrix.

The maximum interfacial shear strength of the fiber-matrix bond was deduced as follows.  $\tau_{AV}$  was plotted against  $L_E$ , as shown in Figure 4. Extrapolation of  $L_E$  to zero length then gives the maximum shear strength of the interface, which is 7.5 MPa. This value for the bonding strength in LDPE is approximately one-half that obtained by Capiati and Porter<sup>4</sup> using HDPE as matrix. The contribution of the frictional stress to the interfacial strength is comparatively low (ca. 10%) for these single polymer composites. The critical aspect ratio  $(L/d)_c$  of the HDPE/LDPE composites is apparently twice that of the HDPE self-composite which is 9. The critical aspect ratio for a fiber embedded in a matrix to a length  $L$  is<sup>11</sup>

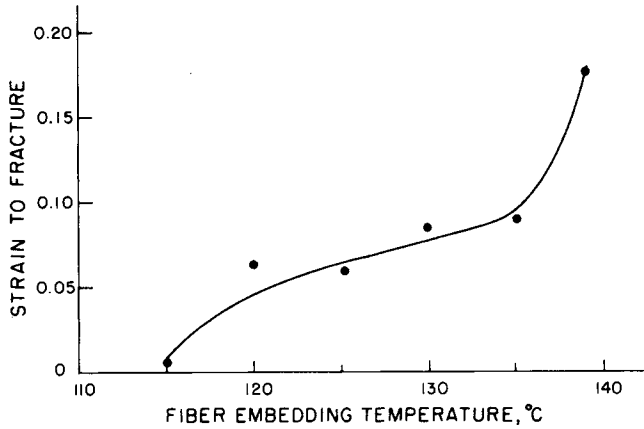


Fig. 3. Strain to fracture of the polyethylene interfacial bonding as a function of fiber embedding temperature. Embedded fiber length is 1 cm.

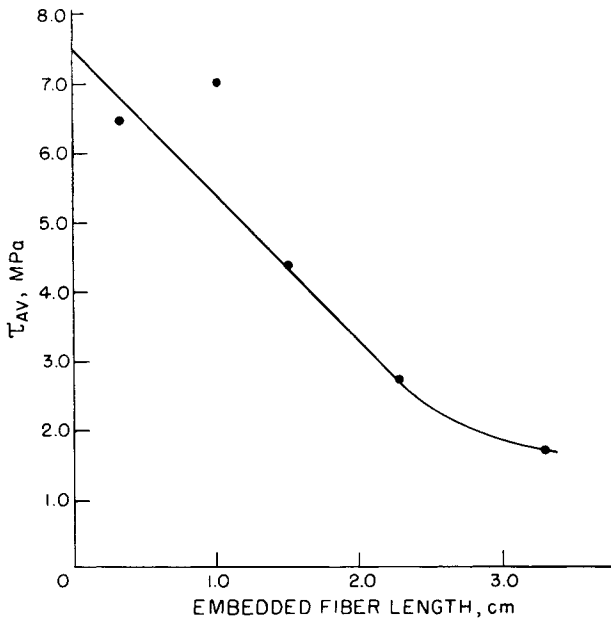


Fig. 4.  $\tau_{AV}$ , the average interfacial shear strength of the polyethylene bonding as a function of the embedded fiber length. Fiber embedding temperature is 130°C.

$$(L/d)_c = (\sigma_F/\tau_{AV})/4 \quad (5)$$

where  $\sigma_F$  is the fracture stress of the fiber. The critical fiber length  $L_c$  for a fiber embedded in the matrix—counting both ends—is  $L_c = \sigma_F/2\tau_{AV}$ .

The derivation of eq. (5) is obtained by assuming the plastic flow model of Kelly and Tyson.<sup>10</sup> Caution must be expressed in the use of this equation in this text.  $L_c$  is the shortest fiber in which the reinforced material fails by fiber fracture rather than by interfacial debonding. However, the majority of deformation tests of the HDPE self-composites and the HDPE/LDPE composites produced interfacial debonding rather than fiber fracture, although deformation of HDPE annealed fibers produced fracture of the fiber core which then separated from

the matrix. By definition of the critical fiber length, the longest fibers capable of surviving in the deformed composite without fracture must be less than  $L_c$ , while fibers exceeding  $L_c$  must fracture.

Capiati and Porter<sup>4</sup> showed the presence of trans-crystalline regions between fiber and matrix using optical microscopy. For HDPE/LDPE composites an intercrystalline region between fiber and matrix was also observed. Further experiments are being pursued to distinguish between the morphology produced by annealing of the fiber surface and epitaxial growth between fiber and matrix.

### Mechanical Properties of Uniaxial Continuous HDPE Film Strips/ LDPE Composites

The modulus variation of the extruded fibers with draw ratio (DR) as a function of the extrusion variables will be reported elsewhere.<sup>9</sup> Figure 5 shows a plot of the modulus variation of the high modulus thin film strip vs DR. The draw ratio variation of the two step or double angle entrance wedge-shaped die may be calculated using the procedure outlined by Capiati et al. for a conical die.<sup>6</sup> Assuming constant volume deformation, then

$$DR = b \left\{ \left[ L^2 \tan^2 \theta_2 + c^2 \left( 1 - \frac{\tan \theta_2}{\tan \theta_1} \right) + \frac{b^2 \tan \theta_2}{\tan \theta_1} \right]^{1/2} - L \tan \theta_2 \right\}^{-1} \quad (6)$$

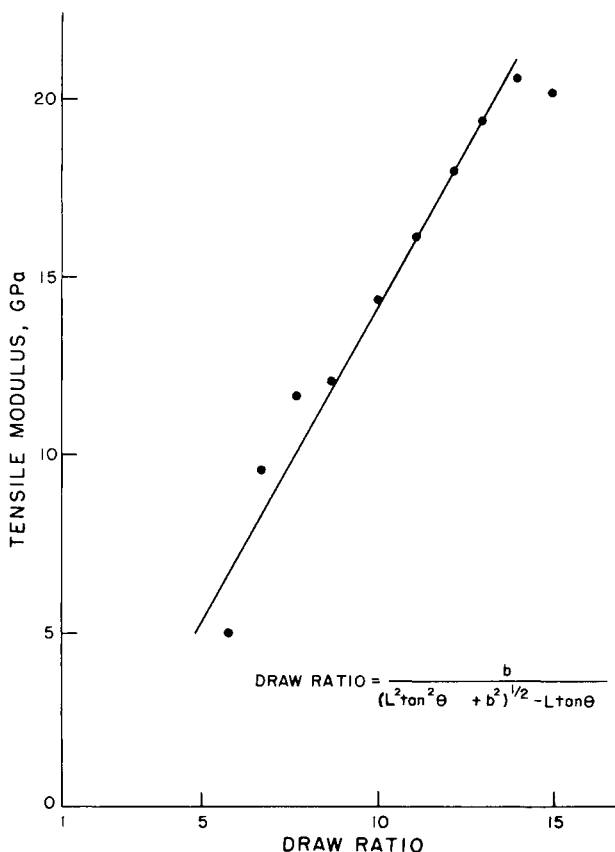


Fig. 5. Dependence of the tensile modulus of a film strip on draw ratio (using a wedge-shaped die with entrance width  $b = 0.8$  cm, decreasing to an inset width of 0.045 cm).  $L$  is the length of the extruded film strip.



where  $L$  is the extrusion length. The DR of the film strip from the single angle wedge-shaped die is given by eq. (6) with  $\theta_1 = \theta_2$  and  $b = c$ , i.e.,

$$DR = b[(L^2 \tan^2 \theta_1 + b^2)^{1/2} - L \tan \theta_1]^{-1} \quad (7)$$

with  $DR = 2b/t < 17.8$ , i.e., provided only HDPE in the die reservoir is extruded. This may be simplified for  $L \gg b$  (providing  $\theta$  is less than  $90^\circ$ ) to

$$DR = 2L \tan \theta_1 / b \quad (8)$$

The modulus variation in the ultradrawn HDPE film strips is therefore proportional to the extrusion length. The maximum modulus of the strips is not as high as for fibers. This is because the draw ratio variation of a wedge-shaped die is a linear ratio of the entrance and die exit dimensions, unlike a cone in which the draw ratio variation is proportional to the square of the ratio of the initial and final die inset dimensions. At a draw ratio of 16, fracture of the thin film strips was observed with the fracture planes perpendicular to the extrusion direction. Apparently, the fracture of the ultraoriented HDPE is not dependent on the absolute modulus, with die geometry determining both the onset of fracture of kink bands as well as the mode of fracture.

In Figure 6 the tensile modulus of the thin film strip is plotted as a function of the extrudate length. The parameter  $V_F$  shown in Figure 6, refers to the

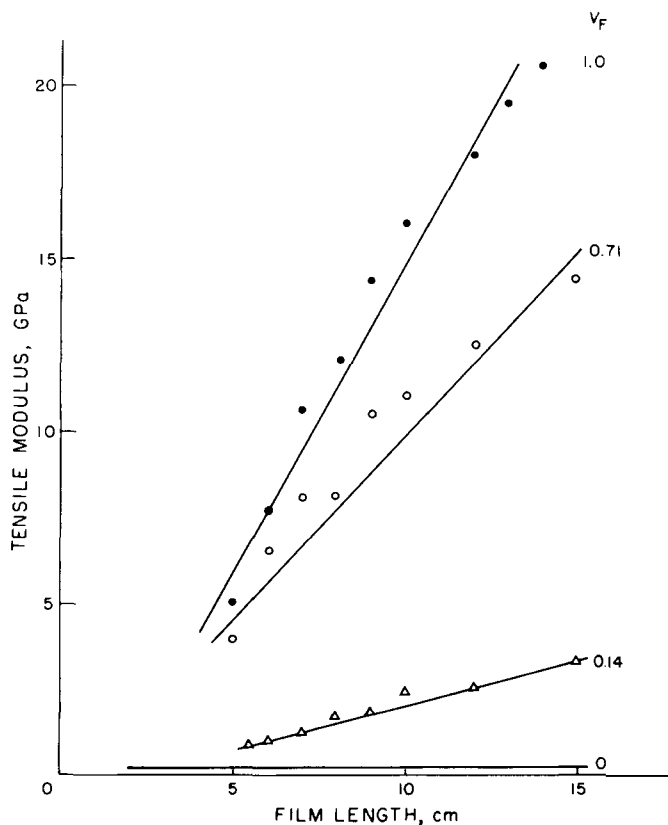


Fig. 6. Tensile modulus of the polyethylene composite as a function of film length at which the modulus was measured.  $V_F$  is the volume fraction of film strip.

volume fraction of film. The ultraoriented HDPE thin films were embedded in the LDPE matrix at several steps of  $V_F$ . The modulus of the composite was again measured using a strain gauge extensometer along the fiber length embedded in the matrix. As  $V_F$  increases the modulus at a given fiber length decreases. The tensile modulus of the composite  $E$  was determined using the cross-sectional area of the composite. The bottom curve in Figure 6, i.e.,  $V_F = 0$ , refers to the matrix modulus. The modulus of the composite is dominated by the fiber modulus.

Figure 6 may be replotted with either fiber length or draw ratio as the parametric variable. In Figure 7 the full lines are drawn according to the simple rule of mixtures,

$$E = V_F E_F + (1 - V_F) E_M \quad (9)$$

where  $E_F$  and  $E_M$  are the fiber and matrix modulus. Equation (9) neglects the term  $V_B E_B / (V_F + V_B)$ , where  $V_B$  is the volume of the bond layer and the corresponding  $E_B$  of 7.5 MPa, the interfacial shear strength of the bond. Equation (9) can be rearranged:

$$E = V_F (E_F - E_M) + E_M \quad (10)$$

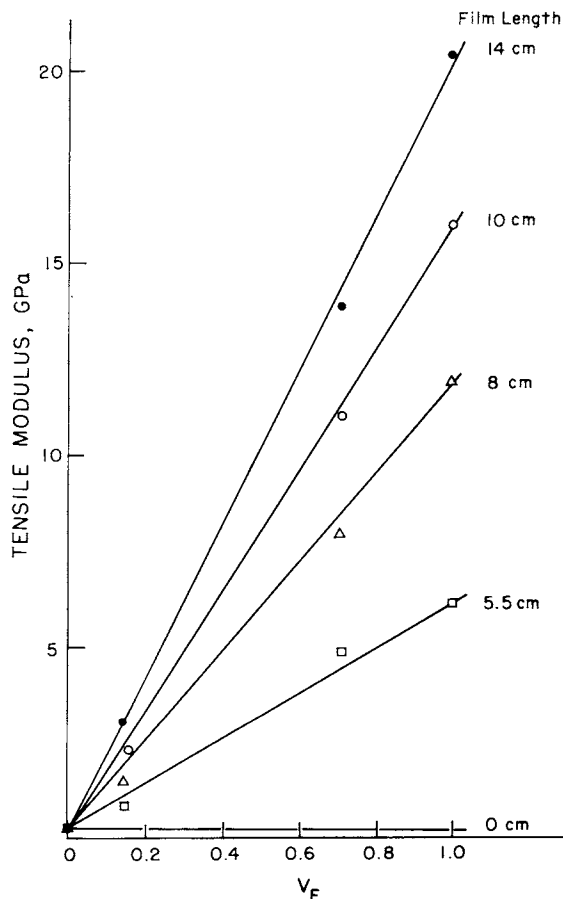


Fig. 7. Tensile modulus of the polyethylene composite as a function of  $V_F$ , the volume fraction of film strip, with the length of the extrudate where the modulus was measured as the parametric variable.

to show that the experimental points in Figure 7 appear to agree with eq. (10).

Figure 8 shows a plot of the tensile strength of the continuous film strip composite vs.  $V_F$ . The ultimate strength of a composite containing uniaxially aligned uniform strength continuous films at a volume fraction greater than a certain critical value can be described in terms of the simple rule of mixtures:

$$\sigma_C = \sigma_F V_F + \sigma_M (1 - V_F) \quad (11)$$

where  $\sigma_M$  is the stress supported by the matrix when the reinforcement fractures and  $\sigma_F$  is the fracture stress of the thin films.

There appears to be some deviation of the data from eq. (11) as shown by the full line in Figure 8. This is most probably due to the less than perfect bonding between matrix and reinforcement. The thin film strips do not have uniform strength.

### Cross-Ply Laminates

The ultraoriented fibers are highly anisotropic as shown by the expansion coefficients parallel and perpendicular to the tensile axis.<sup>9</sup> The longitudinal stiffness is an order of magnitude higher than the transverse stiffness. It may be expected that the tensile modulus of a composite with increasing fiber orientation  $\theta$ , with respect to the tensile axis, will decrease as  $\theta$  approaches  $90^\circ$ .

A ply is a thin sheet of material consisting of an oriented array of thin films embedded in a continuous matrix.<sup>12</sup> To produce a laminate two plies were bonded together with the planar thin films at  $\pm \theta$  to the tensile axis.

Figure 9 shows the variation of the tensile modulus with orientation of the thin

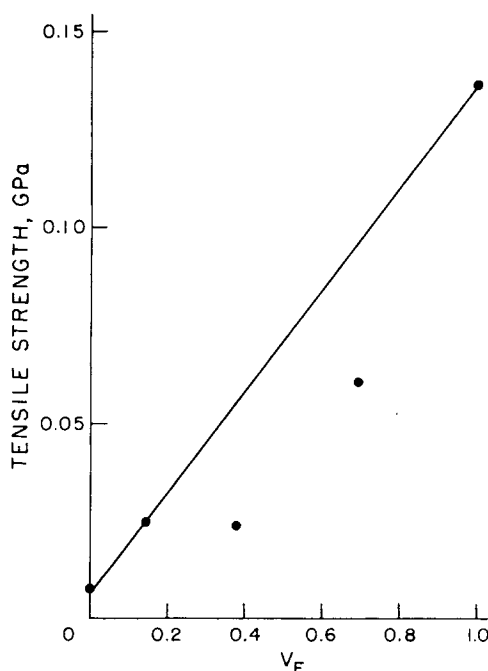


Fig. 8. Tensile strength of the polyethylene composite as a function of  $V_F$ , the volume fraction of film strip. The solid line is a plot of eq. (11) with  $\sigma_F = 0.14$  GPa and  $\sigma_M = 7$  MPa.

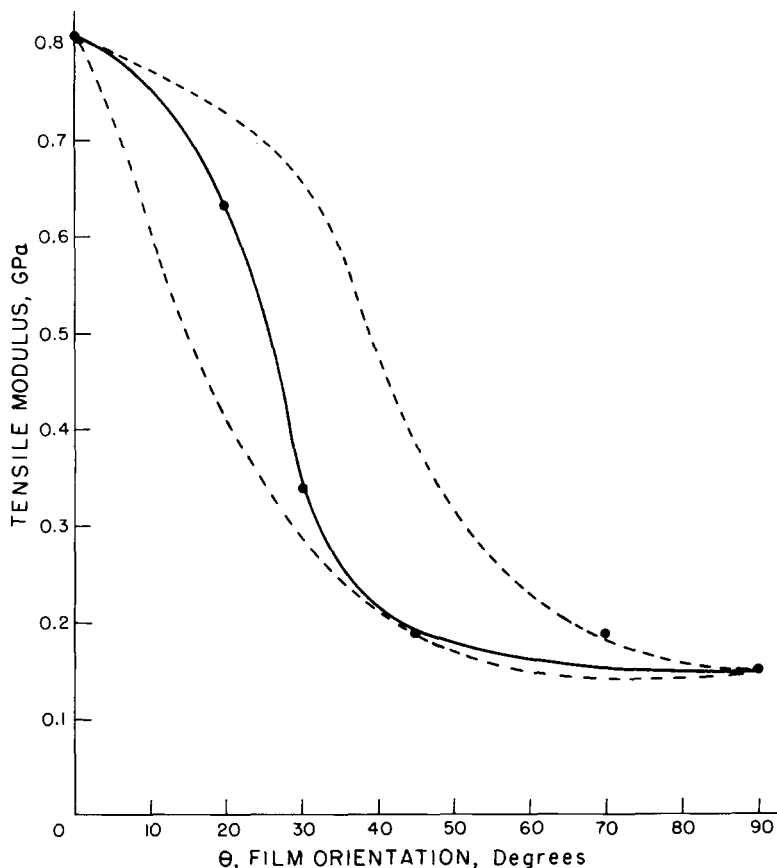


Fig. 9. Tensile modulus of the polyethylene cross-ply laminate as a function of  $\pm \theta$ , the orientation of the film strips with respect to the tensile axis. Dotted lines are plots of eq. (13) with  $E_{11} = 0.81$  GPa,  $E_{22} = 0.15$  GPa,  $\nu_{12} = 0.3$ ,  $G_{12} = 0.31$  GPa (upper bound), and  $G_{12} = 0.25$  (lower bound).

films with respect to the tensile axis. The modulus rapidly decreases with orientation and, when  $\theta$  is  $90^\circ$ , the modulus of the composite  $E_{22}$  approaches that of the LDPE matrix, ca. 0.2 GPa. The value of the transverse modulus of the composite, when  $\theta$  is  $90^\circ$ , may also be deduced from the simple law of mixtures, i.e.,

$$1/E_{22} = (1 - V_F)/E_M + V_F/E_F \quad (12)$$

and  $E_{22}$  ca. 0.2 GPa when  $V_F = 0.1$  and  $E_F$  ca. 10 GPa. When  $\theta$  is  $0^\circ$ , the modulus of the composite is calculated using Eq. (9). The longitudinal modulus should be ca. 1 GPa. The experimental value is slightly less than this. Since a dumb-bell-shaped mold was used, then as  $\theta$  is varied the aspect ratio of the films also varies. The elastic modulus of unidirectional composites with anisotropic filaments has been calculated.<sup>13,14</sup>

The tensile modulus of the cross-ply laminate  $E'_{11}$  as a function of film orientation is given by<sup>14</sup>

$$\frac{1}{E'_{11}} = \frac{\cos^4\theta}{E_{11}} + \left( \frac{1}{G_{12}} - \frac{2\nu_{12}}{E_{11}} \right) \frac{\sin^2 2\theta}{4} + \frac{\sin^4\theta}{E_{22}} \quad (13)$$

where  $E'_{11}$ ,  $E_{22}$ ,  $G_{12}$ , and  $\nu_{12}$  are the principal elastic moduli of the composite and

are the longitudinal stiffness, transverse stiffness, the longitudinal shear modulus, and the major Poissons ratio, respectively. Both  $E_{11}$  and  $\nu_{12}$  follow the rule of mixtures [eq. (15)]. The tensile modulus of the composite when  $\theta$  is zero, or the longitudinal modulus, is 0.81 GPa from Figure 9.  $E_{22}$  is assumed to be equal to 0.15 GPa. Both  $\nu_{12}$  and  $G_{12}$  have not been measured for the ultraoriented filaments. It will be assumed that  $\nu_{12} = 0.3$  although it is possible that  $\nu_{12}$  is far greater than this value because of the high anisotropic behavior of the ultradrawn fibers. The longitudinal shear modulus can be predicted from existing analysis.<sup>15,16</sup>  $G_{12}$  for an isotropic filament is given by  $G_{12} = E_{11}/2(1 + \nu_{12})$ . Thus  $G_{12} = 0.31$  GPa if  $\nu_{12} = 0.3$  and  $E_{11} = 0.81$  GPa. The experimental data in Figure 9 lies between the upper and lower bound dotted lines using eq. (13) with  $\nu_{12}$  equal to 0.3 and  $G_{12}$  equal to 0.31 and 0.25. The tensile modulus vs  $\theta$  has also been calculated as the aspect ratio is varied.<sup>12</sup>

Figure 10 shows the tensile strength of the cross-ply laminates vs.  $\theta$ , the angle the planar thin film strips are oriented with respect to the tensile axis. The tensile strength of the polyethylene composite was determined by the ratio of the maximum stress sustained by the composite before catastrophic failure or film pullout due to debonding to the cross-sectional area of the composite perpendicular to the tensile axis. The volume fraction of film was constant and equal to 0.1.

The tensile strength measurements are markedly dependent on  $\theta$ . The tensile strength of the composites decreases by a factor of  $\sim 5$  as  $\theta$  varies from  $0^\circ$  to  $90^\circ$ . This factor is comparable to the ratio of the tensile strength of the film parallel and perpendicular to the tensile axis. The strength measurements will also be determined, according to eq. (3), by the maximum interfacial shear strength of

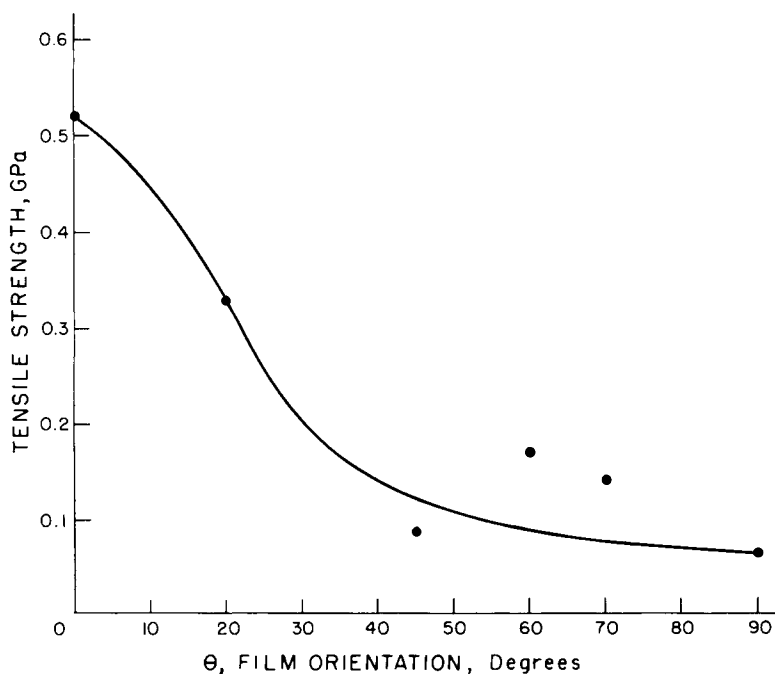


Fig. 10. Tensile strength of the polyethylene composite as a function of  $\pm \theta$ , the orientation of the film strips with the tensile axis.

the composite bonding. As  $\theta$  approaches  $90^\circ$ , the interfacial failure occurs by fracture and separation of the matrix and film. The tensile strength of the composite when  $\theta$  is zero degrees is determined by the law of mixtures, eq. (11). When  $\theta$  is  $90^\circ$ , the tensile strength of the composite will be comparable to the tensile strength of the LDPE matrix. Mathematical treatments that have been used for predicting moduli of cross-ply laminates can also be used for predicting their tensile strengths.<sup>12</sup>

A further composite which can now be evaluated, in view of the orientation study given above, is that of a balanced and symmetrical  $0^\circ/90^\circ$  laminate with two  $0^\circ/90^\circ$  laminates stacked in sequence. The stress-strain behavior of this type of composite has been predicted.<sup>17</sup> A bilinear stress-strain curve is expected up to rupture. Figures 11 and 12 show the stress-strain and fracture behavior of this special type of single-polymer composite.

The initial slope of the  $0^\circ/90^\circ$  composite modulus is the sum through the thickness of the plane-stress stiffness of each layer. As the laminate is deformed, each ply possesses the same in-plane strain and when the strain on the  $90^\circ$  layers reaches the strain level at which ply failure occurs, the  $90^\circ$  layers crack and craze. Separation and fracture of the matrix-fiber bond occurs for the  $90^\circ$  layers. For the  $0^\circ/90^\circ$  construction, the ratio of the ultimate failure stress to the crazing stress is 1.7. The failure of the  $90^\circ$  layers in the laminate prevents the  $90^\circ$  layers from carrying their maximum potential load. This load is transferred by the LDPE matrix to the  $0^\circ$  layers resulting in a loss of laminate modulus. As shown in Figure 11, continual loading ultimately produces failure of the composite when the strain capability of the  $0^\circ$  layers is exceeded and/or the matrix-fiber bond of the  $0^\circ$  layers is sheared. As shown in Figure 11, there is a rapid drop in the load sustained by the composite and the films begin to pull out of the matrix. The strain at which the stress is a maximum in Figure 11 is ca. 0.1 which is comparable to the strain required to produce interfacial failure of the polyethylene composite as shown in Figure 3.

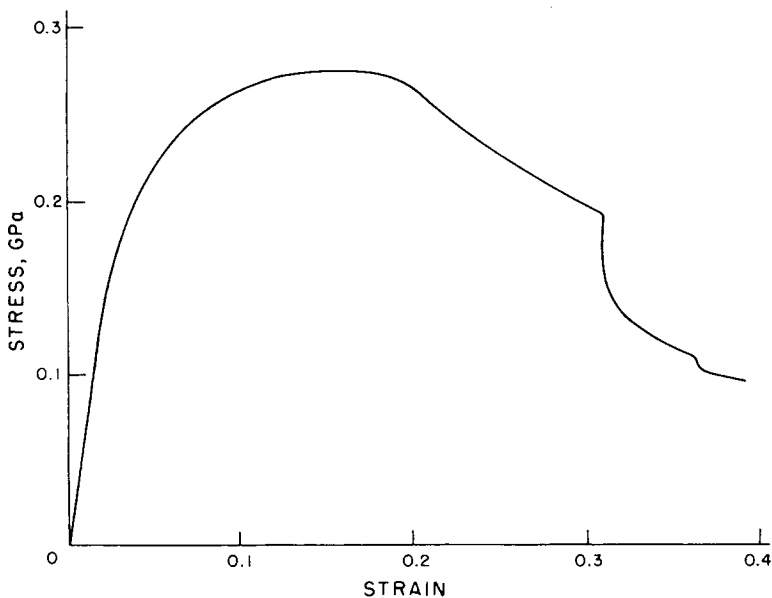


Fig. 11. Stress-strain behavior of the  $0^\circ/90^\circ$  cross-ply laminate.

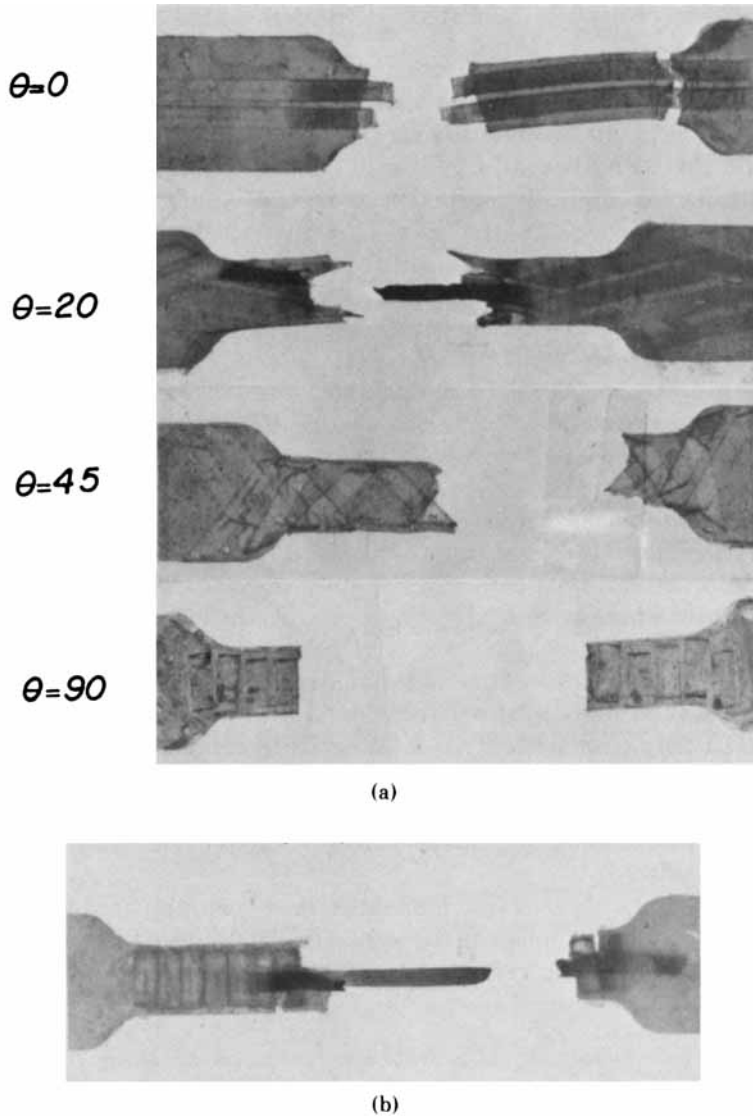


Fig. 12. Fracture behavior of the polyethylene composites.

Figure 12 shows the fracture and crazing behavior of cross-ply laminates with the ultradrawn HDPE film strips embedded in LDPE at  $\pm \theta$  deg to the tensile axis.  $\theta$  varied from  $0^\circ$  to  $90^\circ$ .

In general, as the composites were deformed, crazing and stress whitening of the film strips were observed just prior to fracture of the interfacial bond. From Figure 12 it is noted that fracture occurs near one end of the dumbbell-shaped specimen. Fracture occurred at the low strength part of the film strip. All films were embedded with the low draw ratio section at one end of the dumbbell specimen. The other end of the specimen contained the highest modulus HDPE. Extensive crazing was observed just prior to fracture at the crossover points of each film oriented  $\pm \theta$  to the tensile axis.

## CONCLUSIONS

(i) High strength composites can be prepared using HDPE film strips and fibers embedded in both low- and high-density linear polyethylene.

(ii) The optimum temperature range required for bonding a laterally unconstrained HDPE fiber in LDPE is 130°–132°C. Below 130°C, the bonding is mainly due to compressive shrinkage of the matrix surrounding the fiber. At temperatures above 130°C the fiber is rapidly structurally reorganized with significant modulus reduction. This optimum embedding temperature for maximum interfacial strength should also apply to HDPE as composite matrix, since the bonding properties are determined by the annealing properties of the HDPE and the expansion coefficients of HDPE and LDPE, used in determining  $\tau_{AV}$  according to eq. (3), will be comparable.

(iii) The tensile modulus of the annealed HDPE fibers, which are composites having an ideal gradient of morphology between fiber and matrix, obeys the law of mixtures rule.

(iv) The interfacial shear strength of the bond between HDPE and LDPE is 7.5 MPa. The critical aspect ratio for the HDPE fibers embedded in the LDPE matrix is 18, and this apparently suggests advantageous uses as short HDPE fiber reinforcement where interfacial strength controls the mode of deformation and fracture.

(v) The tensile moduli of the uniaxial and continuous HDPE/LDPE composites obeys the law of mixtures rule, eq. (9).

(vi) The tensile strength of the HDPE/LDPE composites does not appear to obey a simple law of mixtures, eq. (11). This is an indication that the interfacial bonding may not be perfect (possibly due to incompatibility between the HDPE and LDPE), and that further direct methods of assessing the adhesion must be considered.

(vii) High strength cross-ply laminates have been prepared with the mechanical properties dependent on the angle  $\theta$  the HDPE thin films are embedded in the LDPE matrix, according to the stress-strain relations of an orthotropic composite.

The authors are indebted to Dr. M. S. Smith of duPont for generously supplying the Alathon polyethylenes. They also express appreciation for financial support to the Office of Naval Research.

## References

1. N. J. Capiati and R. S. Porter, *J. Polym. Sci.*, **13**, 1177 (1975).
2. J. H. Southern and G. L. Wilkes, *J. Polym. Sci., Part B*, **11**, 555 (1973).
3. W. G. Perkins and R. S. Porter, *Bull. Am. Phys. Soc.*, **AJ10**, 235 (1976).
4. N. J. Capiati and R. S. Porter, *J. Mater. Sci.*, **10**, 1671 (1975).
5. W. T. Mead and R. S. Porter, *J. Appl. Phys.*, **47**, 4278 (1976).
6. N. J. Capiati, S. Kojima, W. G. Perkins, and R. S. Porter, *J. Mater. Sci.*, **12**, 334 (1977).
7. R. G. C. Arridge and M. J. Folkes, *J. Phys. D*, **8**, 1053 (1975).
8. R. S. Porter, J. H. Southern, and N. E. Weeks, *Polym. Eng. Sci.*, **15**, 213 (1975).
9. W. T. Mead and R. S. Porter, to appear.
10. A. Kelly, *Proc. R. Soc. London, Ser. A*, **319**, 95 (1970).
11. A. Kelly and W. R. Tyson, *J. Mech. Phys. Solids*, **13**, 329 (1965).
12. L. Nicolais, *Polym. Eng. Sci.*, **15**, 137 (1975).
13. S. G. Lekhnitski, *Theory of Elasticity of an Anisotropic Body*, Holden Day, 1963.
14. J. M. Whitney, *J. Comp. Mater.*, **1**, 188 (1967).



15. Z. Hashin and B. W. Rosen, *J. Appl. Mech.*, **31**, 223 (1964).
16. C. H. Chen and S. Cheng, *J. Comp. Mater.*, **1**, 30 (1967).
17. J. C. Halpin, *J. Comp. Mater.*, **6**, 208 (1972).

Received May 20, 1977

Revised August 1, 1977